iScience

CellPress
OPEN ACCESS

Review

Biological nanopores for single-molecule sensing

Simon Finn Mayer,[1] Chan Cao,[1] and Matteo Dal Peraro[1,*]

SUMMARY

Evolution has found countless ways to transport material across cells and cellular compartments separated by membranes. Protein assemblies are the cornerstone for the formation of channels and pores that enable this regulated passage of molecules in and out of cells, contributing to maintaining most of the fundamental processes that sustain living organisms. As in several other occasions, we have borrowed from the natural properties of these biological systems to push technology forward and have been able to hijack these nano-scale proteinaceous pores to learn about the physical and chemical features of molecules passing through them. Today, a large repertoire of biological pores is exploited as molecular sensors for characterizing biomolecules that are relevant for the advancement of life sciences and application to medicine. Although the technology has quickly matured to enable nucleic acid sensing with transformative implications for genomics, biological pores stand as some of the most promising candidates to drive the next developments in single-molecule proteomics.

INTRODUCTION

Nanopore sensing was born with the idea of the Coulter counter, a device designed to count red blood cells in fluids. Although the sensing principle has since remained the same, the technique has become much more sophisticated (Kasianowicz et al., 1996). Pore dimensions used to count the specific analyte have changed from microns to nanometers. Applications of nanopore sensing have broadened allowing detection of smaller and smaller entities, including biomolecules as DNA (Manrao et al., 2012), RNA (Garalde et al., 2018), proteins (Huang et al., 2019, 2020; Ouldali et al., 2020; Yusko et al., 2017), as well as metabolites (Galenkamp et al., 2018; Zernia et al., 2020). The commercialization of devices able to sequence long strands of DNA using nanopores stands tall as a serious breakthrough in the field (Cherf et al., 2012; Manrao et al., 2012) and is accelerating the development of precision medicine. However, because the molecules we now aim to analyze would require quasi-atomic resolution, understanding the physics behind their translocation mechanisms at a microscopic level has become a fundamental requirement for further advancing this technology and enhancing its nominal molecular resolution and field of applicability.

In a typical nanopore experiment, two electrolyte-filled reservoirs are separated by a thin membrane that hosts a nanoscale pore; electrodes immersed in each reservoir serve to apply a voltage bias that in turn drives ions through a narrow channel (Figures 1A and 1B). The current resulting from the flow of ions through the channel is measured and its fluctuations (or blockades with respect to the open pore current, I_0) caused by a translocating molecule report features intrinsically related with the molecular structure and translocation mechanism of said molecule (Figure 1C). Key for molecular detection is the nature of the nanopore used in this setting. Advances in inorganic materials and microfabrication have fostered the adoption of solid-state nanopores based mainly on silicon nitrides. One of their main advantages is their stability as they can be used across a wide range of experimental conditions (e.g., voltage, temperature, pressure, pH, ionic strength) (Houghtaling, 2019).

Nature's counterpart, biological nanopores, spontaneously assemble and insert into lipid bilayers and their proteinaceous nature guarantees the reproducibility of their chemical and structural composition. This inherent reproducible geometry is one of their main advantages over solid-state nanopores whose quality is dependent on the resolution of the fabrication technique used. Their pore lumen size can be extremely variable ranging from a few ångström to tens of nanometers (Houghtaling et al., 2018) allowing to tailor their use to the specific sensing task (Figure 1D). Furthermore, biological nanopores allow to finely modulate the electrostatic and steric properties either by selecting *ad hoc* native pores with the required features

[1]Institute of Bioengineering, School of Life Sciences, Ecole Polytechnique Fédérale de Lausanne (EPFL), 1015 Lausanne, Switzerland

*Correspondence: matteo.dalperaro@epfl.ch

https://doi.org/10.1016/j.isci.2022.104145

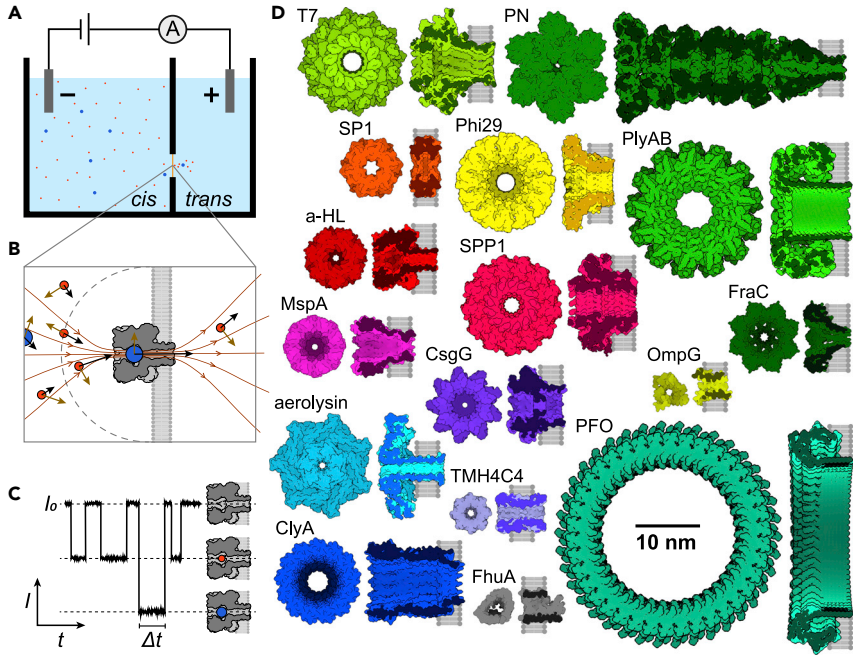

Figure 1. Nanopore sensing using biological pores

(A) Schematic of a nanopore recording setup with two different analytes (red & blue) in an electrolyte solution (light blue) (not to scale). Analytes translocate through a biological nanopore (not shown) in the lipid membrane (orange).

(B) Schematic depicting the capture radius (dotted line), electric field lines (gray), arrows representing random motion (brown) and electrophoretic forces (black) acting on the analyte, quantified by the length of the arrow (not to scale).

(C) Schematic of the ionic current measured in an experiment including open pore current (I_0), the current blockades and dwell times (Δt) associated with translocation of two different analytes with different sizes.

(D) Biological pores used in nanopore experiments (except TMH4C4). Left to right, top to bottom: T7 (light green, PDB code 3J4A), engineered proteasome nanopore (dark green, figure made from the coordinates from ref. 97, credits to G. Maglia), SP1 (orange, 1TR0), Phi29 (yellow, 1JNB), PlyAB (electric green, 4V2T), α-HL (red, 7AHL), SPP1 (magenta, 2JES), OmpG (yellow green, 2JQY), FraC (forest green, 4TSY), MspA (pink, 1UUN), CsgG (purple, 4UV3), PFO (turquoise, 2BK1), aerolysin (cyan, 5JZT), TMH4C4 (lavender, 6M6Z), engineered FhuA ΔC/Δ4L (gray, 1BY3), and 13-meric ClyA (blue, 6MRU), scale bar 10 nm.

or by engineering their structure introducing functional groups or mutations (Cao et al., 2019; Crnković et al., 2021; Robertson et al., 2012).

Thanks to their properties biological nanopore experiments usually present low variability, can be quickly and easily set up and allow to acquire data for several hours (Hanke and Schlue, 1993), whereas their inorganic counterpart have a much larger experimental variability, can be clogged easily (Awasthi et al., 2020), and are not easily wetted. However, biological pores need a lipid bilayer support, which is relatively fragile, limiting the range of conditions one can employ (e.g., voltage, chemical additives, pH, temperature, and external pressure). Although most biological nanopores are stable at different pH, temperature, voltage, and ionic strength, the biological pore itself also limits these experimental conditions. The lateral diffusion of biological nanopores in the lipid bilayer implies that their spatial localization remains ill-defined, which along with the membrane instability complicates their integration with other sensing techniques such as atomic force microscopy or optical tweezers. This combination is possible in solid-state nanopores which can be integrated with techniques such as field-effect transistors, quantum tunneling, fluorescence, and plasmonic sensing (Xue et al., 2020).

Today the catalog of proteins used for nanopore sensing has become vast thanks to the advances of structural biology, which increasingly provides the structures of pore assemblies at atomic resolution. Through this structural knowledge, specific pores can be selected for well-defined applications depending on their geometry and electrostatic properties (Figure 1D). α-Hemolysin (α-HL, in red in Figure 1D) was the first biological pore used for characterization of individual polynucleotides (Kasianowicz et al., 1996) and has since

remained one of the most widely used (Song et al., 1996). Later, α-HL was joined by other pore-forming toxins (Dal Peraro and van der Goot, 2016) (PFTs) such as aerolysin (in cyan in Figure 1D) (Dal Peraro and van der Goot, 2016), a heptameric cytolytic PFT that exhibits a diameter of around 1 nm and a longer pore lumen (~10 nm). The unique features of aerolysin provided an opportunity to study the effect of pore electrostatics on the ion selectivity, ionic conductance, and molecular sensing capabilities (Cao et al., 2019). Bacterial curli transport lipoprotein (CsgG, in purple in Figure 1D), a nonameric peptide transporter (Goyal et al., 2014) also has a narrow pore constriction of ~1 nm that shows a high sensitivity for DNA sequencing (as such it is currently used by Oxford Nanopore Technologies (ONT) in their sequencing devices (Deamer et al., 2016)). *Mycobacterium smegmatis* porin A (MspA, in pink in Figure 1D), is octameric and follows with 1.2 nm at the narrowest constriction. This pore has a funnel geometry providing a better sensing resolution for biopolymers like DNA or proteins (Butler et al., 2008). The engineered ferric hydroxamate uptake component A mutant (FhuA ΔC/Δ4L, in gray in Figure 1D) also features a constriction of 1.2 nm (Niedzwiecki et al., 2012) and unlike most other pores is monomeric. Sea anemone derived fragaceatoxin C (FraC, in green Figure 1D) is octameric and also exhibits a funnel geometry with the narrowest point being 1.6 nm (Wloka et al., 2016). By further engineering, FraC can be isolated in its heptameric and hexameric assembly which reduces the diameter to 1.1 and 0.84 nm, respectively (Huang et al., 2019). Engineered FraC pores are also able to capture both positively and negatively charged peptides, which is crucial for nanopore protein analysis (Huang et al., 2017). The 12-meric plant derived boiling stable protein 1 (SP1, in orange in Figure 1D) has an opening of 3.0 nm (Wang et al., 2013a) and exhibits an unusually short channel of 5.0 nm. Similarly, the viral derived SPP1 DNA packing motor (in magenta in Figure 1D) has an opening of 3.0 nm (Zhou et al., 2016). Following in size is the PFT Cytolysin A (ClyA, in blue in Figure 1D) which in its 12 to 14-mer conformation has a 3.3 to 4.2 nm constriction at the very end of the pore and exhibits a large vestibule before the constriction beneficial for trapping analyte; it was the first biological nanopore used to host a fully folded protein (Soskine et al., 2013). In a similar size range, the viral derived 12-meric connector of the Phi29 DNA packing nanomotor (in yellow in Figure 1D) and the channel of bacterial virus T7 DNA packaging motor (T7 in green in Figure 1D) exhibit constrictions of 3.6 nm (Wang et al., 2013b) and 3.9 nm (Ji and Guo, 2019) respectively. The fungus derived pleurotolysin (PlyAB, in green in Figure 1D) has one of the largest channels with a 5.5 nm constriction, the pore is oligomeric and has two components: PlyA that recruits PlyB to the membrane, which spans the bilayer (Huang et al., 2020). One of the biggest biological nanopores is the cholesterol dependent cytolysin Perfringolysin O (PFO in turquoise in Figure 1D), which has an opening of approximately 25 to 30 nm depending on its multimeric state (Johnson and Heuck, 2014) and might be used in the future for the detection of much larger analytes. Although translocation data has yet to be presented, the completely *de novo* designed TMH4C4 (Xu et al., 2020) pore (in lavender in Figure 1D) serves as an impressive first example of a fully synthetic pore not yet explored by evolution and built *in silico* from scratch. Despite the fact that a continuous non-gating conductance is essential in most nanopore sensing approaches, some membrane channels exhibiting a frequent gating have also been used as biological nanopores for protein sensing; for example, the monomeric β-barrel outer membrane protein G (OmpG, in yellow green in Figure 1D), which can directly discriminate antibodies from serum samples thanks to the distinct gating patterns (Fahie et al., 2015).

ptOur aim in this review is to give an overview of the problems associated with nanopore sensing when using these biological nanopores and provide guidance on how these problems can be resolved or circumvented. Furthermore, we will discuss how the sensing properties of this repertoire of biological pores have recently been exploited to advance single-molecule analysis applied to biological and medical applications.

PROBLEMS ASSOCIATED WITH BIOLOGICAL NANOPORES AND RELATIVE SOLUTIONS

The most important parameter in nanopore sensing is the ionic conductance ($G = I/V$) measuring how well the ionic current flows through the pore depending on the electrolytes conductivity, the pore diameter and its length (Kowalczyk et al., 2011). A large conductance is often preferable as a lower applied voltage results in larger signals. Conductance can be experimentally determined measuring ionic currents at different applied voltages, usually using silver/silver-chloride (Ag/AgCl) electrodes in chloride-containing electrolytes. They ensure a faradaic charge transfer and prevent capacitive effects of plain silver: the electrode with applied negative bias will release a chloride ion into solution, whereas the opposite will take up a chloride ion from solution thus injecting one electron into the circuit.

It is then important to understand how analytes translocate through a nanopore. The mobility of analytes is mainly driven by diffusion, and only when the electrophoretic force overcomes the thermal motion the

charged analyte will be driven through the pore (Figures 1A and 1B). This boundary at which thermal motion is equal to the electrophoretic pull on the particle of interest is called the capture radius (Wanunu et al., 2010) (Figure 1B). In the case of electrophoresis driving the translocation, the capture radius is inversely proportional to the length of the pore and proportional to the applied voltage and the pore diameter (Wanunu et al., 2010). Regardless of analyte charge, the electroosmotic flow (EOF) can also be used as the driving force for capture. This flow is caused by the interaction of the applied electric field with the net mobile charge formed when the pore wall is highly charged. The magnitude of EOF depends mainly on the charge of the channel walls as well as the pore length and diameter (Bonome et al., 2017).

In general, EOF, conductance and pore-analyte interactions can vary a lot depending on which pore is used. Moreover, the size of the nanopore determines the analytes that can be detected as they should have similar size to the pore's narrowest constriction to cause a significant and specific reduction of current when translocating. During translocation the analyte modulates the current by taking up space in the nanopore that is otherwise filled with ions (Figure 1C). The volume of the analyte is however not the only feature that modulates the current, as shape, charge, diffusion coefficient, pore-analyte interactions, and position inside the nanopore channel also influence the current (Yusko et al., 2017). All these parameters which complementarily affect the current readout make the interpretation of nanopore sensing experiments far from trivial, involving mechanisms that have yet to be fully understood.

Analyte capture and translocation frequency

To sense a given analyte, it is required (i) to bring it close to the nanopore, and (ii) to capture, that is, confine it within the narrow pore which is energetically unfavorable. The former step is diffusion limited and the entropic barrier of the latter is overcome by the application of a force allowing the analyte to enter the nanopore (Figure 1B). Electrophoretic forces which are commonly used work very well for charged analytes like nucleic acids; the application of pressure works regardless of the electrostatic nature of the analyte but direct application of pressure through compression is not easily applicable to lipid membrane supported nanopores due to their fragility. EOF, like pressure (Lan et al., 2011), is an alternative strategy generating enough drag force to capture analytes (Huang et al., 2017). Following capture, the analyte can exit the nanopore towards the *trans* compartment producing an actual translocation event. If the analyte returns to the *cis* chamber, the mode of sensing is commonly referred as trapping.

The capture needs to be frequent enough (Figure 2A) to collect data reporting on the analyte properties. A low capture rate (Figure 2B) can be especially problematic for the detection of molecules that are present at very low abundance in the sample. Because detection of low abundance biomarkers is of high interest for early diagnostics (Jarockyte et al., 2020; Timp and Timp, 2020), numerous strategies are available to enhance analyte capture rates. The use of asymmetric salt conditions in which the ionic strength in the *trans* chamber is greater than in the *cis* chamber was first introduced in solid-state pores (Wanunu et al., 2010) and later in biological nanopores with the aim of increasing translocation frequency. In α-HL the use of 1 M / 3 M (*cis* / *trans*) NaCl reportedly increased the capture rate by 5.8 fold so that detection of the peptide of interest was possible at a concentration as low as 2.88 pM (Chen et al., 2019); 0.2 M / 3 M KCl allowed the detection of cancer associated microRNA at a concentration of 0.1 pM (Wang et al., 2011); a 0.5 M / 4 M asymmetric KCl solution increased the capture rate of microRNA by 60-fold (Ivica et al., 2017). The rationale behind an increase in capture rate through a salt gradient has been thoroughly examined only for solid-state nanopores (Wanunu et al., 2010). Different ionic species can also influence the capture of analyte as shown for ssDNA in LiCl (Hu et al., 2019). Even though geometry, size and charge of biological nanopores are different, similar observations should hold for them as well.

Another strategy to increase the capture rate is the use of macromolecular crowding, which mimics conditions usually encountered in cells by using synthetic crowders like polyethylene glycol (PEG) or dextran that can be added either to the *cis* (Yao et al., 2020) or *trans* (Chau et al., 2020) compartment or to both (Larimi et al., 2019). Although the mechanism is not completely understood, crowding induces an excluded volume effect on analytes, which leads them to adopt their most compacted state. Moreover, when crowders are similar or bigger in size than analytes, their diffusion follows anomalous behaviors by which the mean square displacement of the analyte scales sublinearly over time, as observed in the cellular environment (Chau et al., 2021; Woringer et al., 2020). Both these effects influence the binding affinity of the pore and analytes, an effect that is called depletion interaction in-depth discussed in ref (Chau et al., 2021) and observed when PEG crowders were used to study the translocation of a 23 amino acid-long peptide

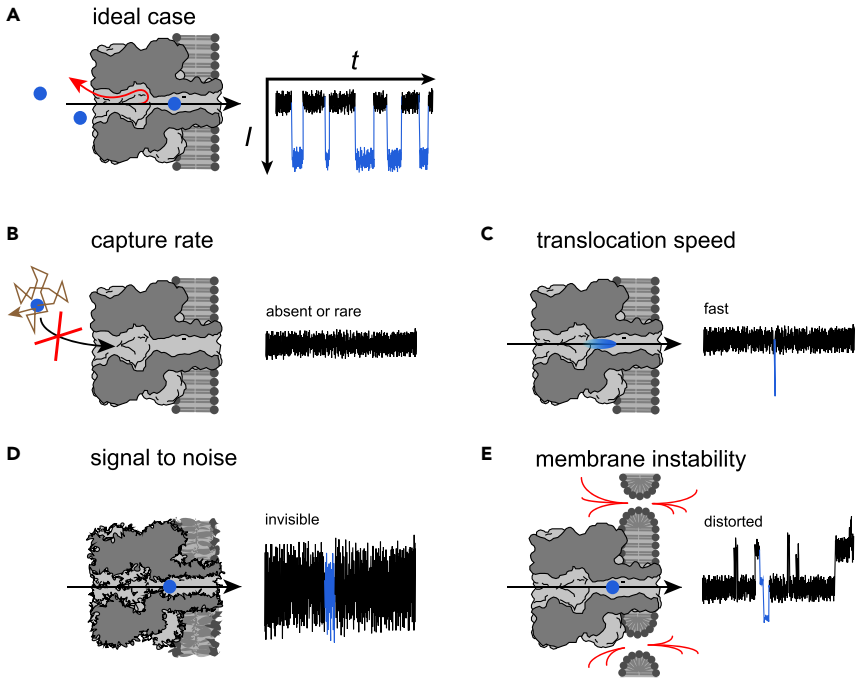

Figure 2. Significant problems associated with biological nanopore experiments

(A) Ideal case: frequent translocation events separated well from the open pore current. Trapping events are also indicated by the red arrow returning to the *cis* chamber.

(B) Capture rate: the analyte (blue) does not enter the nanopore because of low abundance or a lack of driving force.

(C) Translocation speed: the analyte passes the nanopore too fast and produces a signal that is not well resolved; i.e., not enough datapoints are collected.

(D) Signal to noise ratio: the noise caused by the experimental setup, membrane or pore is so high that the translocation of the analyte is not clearly distinguishable from the open pore current.

(E) Membrane instability: the ionic current flows not only through the pore but also through transient channels in the unstable membrane causing the translocation event to be distorted.

through α-HL. They found a 7-fold increase in event frequency and a 2-fold increase in dwell time when using PEG 4000 at 25% w/v. Also using α-HL, Yao et al. have recently reported a 25-fold increase in translocation frequency for single strand DNA and an almost 6-fold increase in dwell time using a crowding solution of PEG 4000 at 40% w/v exclusively on the *cis* chamber (Yao et al., 2020). Another possibility for affecting the capture rate of analytes is the use of different cations, as observed for ssDNA longer than 100 nucleotides which could be captured by aerolysin pores with a 10-fold enhanced capture rate by using LiCl electrolyte (Hu et al., 2019).

When the analyte is not charged it cannot be electrophoretically driven through the nanopore. The charge can either be introduced through chemical modification of the analyte (Nivala et al., 2013; Ouldali et al., 2020; Rosen et al., 2014), the adjustment of the electrolyte's pH (Huang et al., 2019) or the EOF can be used for enhancing capture. Similar to the capture radius generated by an electric field one can think of a radial distance from the nanopore at which the flow-induced drag force overcomes the random motion and the analyte molecule moves towards and eventually through the nanopore. In biological nanopores a sufficient EOF is mostly generated through engineering proper electrostatics into the pore lumen or simply by conducting the experiment at a low or high pH (Asandei et al., 2016; Huang et al., 2019; Wang et al., 2017b) at which the overall charge of the pore will be more positive or negative, respectively. The EOF can in some cases be large enough to capture analytes against the electrophoretic force (Asandei et al., 2016) and be used to capture peptides and proteins in α-HL (Asandei et al., 2016), FraC (Huang et al., 2019), MpsA (Liu et al., 2022), and PlyAB (Huang et al., 2020). In addition, the introduction of pore mutations contrasting the electrostatic signature of the analyte is also a solution to increase the capture rate (Maglia et al., 2008). For example, tethering the molecule of interest to the membrane can increase the capture

rate, a strategy first used in solid-state nanopores (Yusko et al., 2011) and later adapted for biological pores (Brinkerhoff et al., 2021; Laszlo et al., 2014). Another way to increase capture frequency is signal amplification. Instead of directly detecting the molecule of interest itself a second species which is more abundant is detected which provides quantitative information about the analyte (Kwak et al., 2020) or simply reports if an analyte is present or not (Xi et al., 2018).

Translocation speed

Molecular information about the analyte is collected in the form of current readout during the time it spends within the nanopore. Therefore, the duration of the translocation events needs to be significantly longer than the time resolution of the recording equipment. Depending on pore and analyte, translocation typically occurs on the millisecond timescale and data are collected at 100 kHz, i.e., with a temporal resolution of 10 μs. Thus, maximizing the amount of information in each recorded event translates to prolonging the residence time within the nanopore. Often the translocation of analytes is too fast for productive measures (Figure 2C) thus several strategies have been developed to decrease translocation speed mainly relying on a trade-off for a reduction in translocation frequency or signal to noise ratio. Macromolecular crowding, as mentioned before, can slow down translocation through an increase in viscosity of the medium caused by the crowding agents. Such strategies were used to reach a 6-fold increase of dwell time without a significant reduction of the signal to noise ratio (Yao et al., 2020). Media that have a higher viscosity without a decrease in conductivity such as ionic liquids have also been shown to be compatible with OmpF (Modi et al., 2011) and α-HL increasing the dwell time of single stranded DNA significantly (de Zoysa et al., 2009). Demonstrations of the use of ionic liquids remain sparse and the cause of the increase in dwell time needs to be investigated further. Asymmetric salt as well as the use of Li ions has been shown to slow down translocations in solid-state nanopores (Kowalczyk et al., 2012; Wanunu et al., 2010) and biological nanopores for Li (Boukhet et al., 2016; Ivica et al., 2017) and Cs (Ivica et al., 2017). The pore geometry can also play an important role in modulating the residence time: in aerolysin two consecutive constriction sites create a vestibule (Cao et al., 2018), which allows for prolonged residence time of peptides below a certain size (Piguet et al., 2018). This residence time can further be prolonged by increasing the affinity between the pore and analyte through mutations that introduce electrostatic interactions (Li et al., 2020b). This is demonstrated also in the approach of Chavis et al. that produced a 2-fold increase in the residence time of short cationic peptides in α-HL, by trapping a negatively charged thiolate capped gold clusters (2 nm) inside the vestibule of α-HL (Chavis et al., 2017).

Instead of fully translocating analytes it can be relevant to indefinitely trap them within the nanopore by the use of electrophoresis (Galenkamp et al., 2020), EOF (Asandei et al., 2016; Huang et al., 2020), their interplay (Zernia et al., 2020) or the addition of a bulky molecule at one end, like streptavidin (Purnell and Schmidt, 2009; Stoddart et al., 2009). These translocation stoppers, which can be designed in a controlled way based on the geometry of the pore, do not completely hinder the flow of ions so that the signal to noise ratio is still sufficient to gather information about the analyte. These methods report observation times of analytes inside of the pore of several seconds (Van Meervelt et al., 2017; Zernia et al., 2020).

When working with high information density polymers like DNA and proteins, slowing translocation down is of crucial importance. In these cases, motor proteins that bind DNA or proteins can be used to slowly feed the analytes through the nanopore (Lieberman et al., 2010). Phi29 DNA polymerase has been early adopted as the main motor protein employed for DNA reading and without this gain in translocation control, DNA sequencing would not have been possible as implemented today. Proteins are more challenging, a universally applicable motor protein has yet to be found and the only demonstrations rely on protein-DNA hybrid molecules that can then be slowed down with helicases (Brinkerhoff et al., 2021) or polymerases (Yan et al., 2021).

Signal and signal to noise ratio

Noise, i.e., statistical fluctuations of the measured current (Figure 2D), is caused by multiple phenomena. The frequency (f) dependent *1/f* noise is the governing noise source at low frequencies (<100 Hz) in biological nanopores. *1/f* noise is not well understood but proposed to be caused by protonation and deprotonation of ionizable sites, changes in ion mobility, rearranging of charges at the pore or other thermally activated processes like conformational changes, or the formation of air bubbles (Fragasso et al., 2020). Temperature dependent noise and current dependent shot noise contribute to midfrequency noise (approximately 0.1–2 kHz), while dielectric and capacitive noise makes up the high

frequency noise (2–100 kHz). Dielectric noise scales linearly with the frequency and depends on the material of the membrane support and membrane (Fragasso et al., 2020). Since Teflon has a low dielectric constant this noise's main contributor is the lipid bilayer. Capacitive noise scales quadratically with the frequency instead and depends on the capacitance of the setup (i.e. amplifier, support and bilayer capacitance) (Fragasso et al., 2020).

To maximize the signal to noise ratio every setup should be carefully optimized, but in many cases the optimization is a tradeoff: for example, increasing voltage compromises bilayer stability, reducing bilayer area decreases the likelihood of pore incorporation and of having a true bilayer (i.e., a bilayer without organic solvent residue thickening it), and reducing the temperature decreases conductivity and capture rate (Payet et al., 2015). Noise arising from the pore itself can be mitigated by mutations or deletions. Adapting the nanopores' size is also a common strategy to increase the signal to noise ratio, because a 1 nm^3 analyte will produce for instance a larger signal in a 1.5 nm wide nanopore than in a 3 nm nanopore. The pores diameter itself can also be widened or narrowed by mutations of the pore lumen (Cao et al., 2019) or at the subunit interface to promote the formation of specific multimer states (Huang et al., 2019). Pores that exist at different stoichiometries can be triggered to assemble into different multimeric states selectively (Fennouri et al., 2021) or be purified by native PAGE (Soskine et al., 2013). Adapter molecules that enter the nanopore and bind inside can also be used to reduce the pores diameter and properties (Wu et al., 2007; Zhang et al., 2021b). Not only the diameter but also the length and geometry of nanopores are of interest because when reading polymers like DNA or proteins, all units (i.e., bases or amino acids) that are in or close to a nanopore constriction at a given moment contribute to the observed electrical signal, complicating its interpretation. Even if the pore were to be truly two dimensional, the resolution would still be imperfect. This is because the current measured with a nanopore is modulated even before the analyte enters and after it exits the pore (Hall, 1975). Another problem is the thermal motion moving the polymer stochastically up and down in the nanopore faster than the commonly used temporal resolution of 10 μs causing a blurring effect. The geometry of MspA is a prime example of reading resolution because the pores diameter expands quickly in both directions after the very short and narrow (0.6 × 1.2 nm) reading site (Laszlo et al., 2013). Such funnel geometry, also exhibited by FraC (Huang et al., 2019) is ideal for polymer sequencing.

Membrane instability

The lipid bilayer constitutes the main weak point when using biological pores for nanopore sensing, its stability is a vital priority thus that other experimental conditions are in turn affected by this requirement, especially the applied voltage, electrolyte conditions and chemical additives that can be used. A typical painted or folded phospholipid bilayer can be used to record at voltages up to around 200 mV. Above this critical voltage, which can differ depending on the experiment's parameters, electroporation occurs and manifests itself in transient leak currents (Figure 2E), which compromise any recorded data. In addition, the use of membrane interacting chemicals such as organic solvents is not compatible with membranes. Several efforts have been taken to improve on this aspect. Better support structures for lipid bilayers like the recently introduced pillars-on-wedge support capable of sustaining lipid bilayers at 350 mV (Kang et al., 2019) are one option. Replacing the lipids entirely by more robust copolymers is an alternative strategy. Yu et al. have recently shown that decane-painted amphiphilic diblock copolymer (PBD-PEO) membranes remain impermeable to ions up to 350 mV and have a longer lifetime than 1,2-Diphytanoyl-sn-glycero-3-phosphocholine (DPhPC) bilayers while still allowing pore incorporation as reported for α-HL and MspA. Further the used copolymer tolerates guanidinium chloride (GdmCl) concentrations of 5 M, whereas DPhPC bilayers can only be reasonably used at concentrations of 1–2 M depending on the recording voltage (Yu et al., 2021). Hybrid pores that use a solid-state nanopore support with a biological nanopore as the sensing element are alternative solutions that have recently been reported (Cressiot et al., 2018; Hall et al., 2010). Another strategy to increase the bilayer stability is by encapsulating it in a hydrogel from both sides (Kang et al., 2007) or by anchoring it to a hydrogel on only one side (Malmstadt et al., 2008).

Pore misbehavior

Although the chemical variability in biological nanopores is much lower than in solid-state nanopores, some pore perturbations can still occur even in cases where the biological pore can be handled and produced well. These variations manifest in an altered open pore current or abnormal current fluctuations. Such pores are usually discarded directly during the experiment through reforming of the membrane. However, if pore-to-pore variation is a problem, careful purification protocols and homogenization with a

thermal annealing protocol can mitigate it (Rodriguez-Larrea, 2021). Another pore related problem that can arise is gating, a behavior that is poorly understood but observed in almost all biological nanopores used in the field (Fahie and Chen, 2015; Huang et al., 2017; Ivica et al., 2017; Kwak et al., 2020; Manrao et al., 2012; Wang et al., 2013b) and characterized by spontaneous stochastic fluctuations of current and complete or partial blockades. This effect could be because of the presence of hydrophobic contaminants present in the electrolyte and is reported to be reduced through filtering with activated charcoal (Lucas et al., 2021b). We have observed this gating behavior to be enhanced in some aerolysin mutants when using asymmetric salt conditions, an observation that has previously been mentioned also for α-HL (Ivica et al., 2017). As for pore-to-pore variation, pore gating can be distinguished from signal, but may be detrimental to an experiment if persistent.

Signal processing and interpretation

Owing to the large heterogeneity of current readouts collected using different nanopores in multiple conditions, there is still a lack of consensus in protocols used for processing signals and therefore in their ultimate interpretation. Commonly, after data acquisition recorded current traces are segmented and selected, i.e., segments of open pore current with e.g., unusually high noise are discarded. Then relevant events are extracted from the selected segments and further analyzed (Plesa and Dekker, 2015). A summary of different analysis techniques applied to solid-state nanopores is given for instance by Plesa and Dekker (2015). Generally, signals above a certain threshold of current blockade and dwell time are regarded as a successful entry into the nanopore. For electrophoretically driven molecules translocation can be proven by a decrease in dwell time when increasing the applied voltage. Apart from the depth of the blockade (generally described as the ratio of the average current of the event and the open pore current, I/I_0), the dwell time and inter-event times, which represent the capture frequency, can be easily extracted. In an in-depth analysis, each event is investigated and features like the root mean square (RMS) noise, the ratio of minimum and maximum (Yusko et al., 2017), identification of different current levels as well as shape description factors are extracted. Since nanopore experiments create large datasets artificial intelligence has been used successfully for the accurate, automatic and unbiased interpretation, classification and prediction of current signals in solid-state (Díaz Carral et al., 2021; Misiunas et al., 2018; Taniguchi et al., 2021) or biological nanopores (Cao et al., 2020; Ni et al., 2019; Smith et al., 2020; Teng et al., 2018).

In addition, the interpretation of the specific signal shape remains a delicate task, demanding carefully designed control experiments to further back up interpretations. In this context, molecular modeling and simulations of pore translocation at atomic resolution have proven useful to interpret the current readouts (Aksimentiev and Schulten, 2005; Kutzner et al., 2011; Mathé et al., 2005). This approach has steadily grown thanks to the improvement of hardware capabilities, molecular force fields, and new computational approaches (Wilson et al., 2019), and today can deliver important insights into the molecular determinants of pore translocation, as shown in recent examples applied to FraC (Lucas et al., 2021b), MspA (Brinkerhoff et al., 2021) and aerolysin (Cao et al., 2019; Ouldali et al., 2020). In addition, to assess larger sizes and timescales, multiscale approaches ranging from the use of coarse-grained models (Zhang et al., 2021a) to continuum mean-field calculations (Willems et al., 2019) are also contributing to guide our understanding of novel pore systems.

SENSING BIOMEDICAL RELEVANT MOLECULES WITH BIOLOGICAL NANOPORES

Nucleic acid sequencing with commercial platforms

DNA was the first analyte of interest for nanopore sensing (Figure 3A): thanks to its uniformly charged phosphate backbone and the relatively low degree of complexity (i.e., 4 bases, ignoring epigenetic modifications), it is ideal for nanopore sensing. DNA and RNA sequencing was thus first developed using biological nanopores and the technology was first made commercially available by ONT in 2015 (Deamer et al., 2016). This technology has become very competitive versus the well-established next-generation sequencing approaches, owing to the low cost, long-read capability, and pocket size (Pennisi, 2016). It is applicable for direct DNA and RNA sequencing of biological samples identifying bacteria, viruses, splicing variants and transcriptional state of an organism without the need for reverse transcription or amplification (Garalde et al., 2018). It has been used to sequence full viral genomes (Keller et al., 2018) while gaining novel insights into structural variants and RNA modifications (Kim et al., 2020; Viehweger et al., 2019). Also, easy and fast detection of viruses like SARS-CoV-2 (Wang et al., 2020) or bacterial meningitis in cerebrospinal fluid (Moon et al., 2019) was recently possible, exploiting the capability of this commercial nanopore sequencing system.

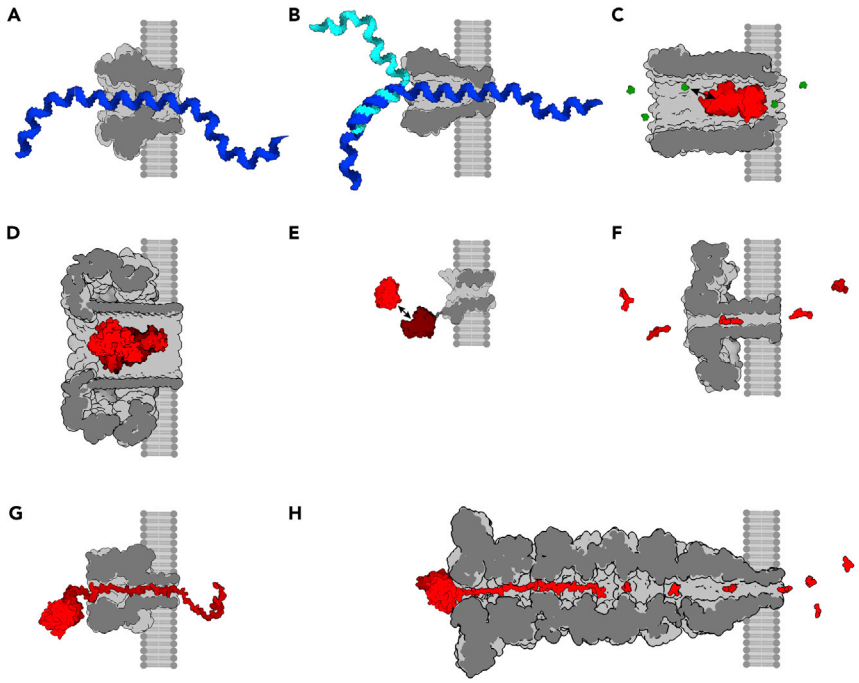

Figure 3. Biological and medical applications of biological pores

(A) Nucleic acid sequencing with CsgG.

(B) Nucleic acid sensing through unzipping probe (cyan) with MspA.

(C)Metabolite (glucose, green) sensing with a trapped adaptor protein (glucose binding domain, red) in ClyA.

(D) Folded protein sensing with PlyAB.

(E) Protein-protein interaction sensing through a OmpG nanopore fused to one of the proteins of interest.

(F) Short peptide sensing with aerolysin.

(G) Protein sensing through unfolding by force with α-HL.

(H) Exopeptidase-based protein unfolding, cleaving and sensing with an engineered proteasome nanopore (figure made from the PDB coordinates of ref. 97, credit to G. Maglia).

Sensing of nucleic acids

Besides nanopore sensing using commercial platforms several parallel efforts exist to expand the sensing capabilities and range of applications of biological nanopores for nucleic acids readout. Van der Verren et al. have recently introduced an adapted CsgG nanopore by including a truncated variant of the CsgF protein, one of CsgG's binding partners. The truncated CsgF holds a constriction itself and upon binding to CsgG the two form a double-constriction nanopore exploited to read short homopolymers with unprecedented accuracy (Van der Verren et al., 2020). Instead of focusing exclusively on current readout, unzipping times of target DNA (Figure 3B) have been measured for the detection of point mutations in oligonucleotides (Liu and Kawano, 2020) using pores like α-HL that can accommodate single stranded but not double stranded DNA (Kasianowicz et al., 1996). The degree of methylation in short DNA fragments was found also to be related to unzipping times (Wang et al., 2017a). Likewise, hybridization probes can also be used to trap single stranded DNA, significantly prolonging the translocation time of the target. This approach has been used to detect epigenetic modifications of cytosine by observation of the base-flipping dynamics at a mismatch site that is identified by the hybridization probe (Johnson et al., 2017). The identification of 3′ versus 5′ phosphorylation in a 40-nucleotide poly-A sequence (Li et al., 2020a) served as an example of the subtleties that can be detected using this approach. Besides these proof-of-principle studies on short sequences several investigations aim at a more direct clinical application, as in the case of detection of lung cancer associated microRNAs in patients (Wang et al., 2011), and highly conserved promoters of influenza A virus in the presence of fetal bovine serum (Oh et al., 2019).

Another α-HL based assay has been recently developed to detect SARS-CoV-2 specific IgG and IgM antibodies indirectly through DNA probes (Zhang et al., 2021c). The assay detected IgG at a detection limit of 10 ng/mL and IgM antibodies at 50 ng/mL, performing better than commercial ELISA and LFA kits

(Zhang et al., 2021c). Another interesting example is the development of a drug screening platform based on riboswitch RNAs, which, when binding to a specific drug can change conformation, exhibiting an intermediate state which is partially single stranded and can be detected in α-HL pores. Although it is still unclear whether this method can provide precise information about drug affinity, three new compounds binding to a riboswitch aptamer domain have been discovered and in the future this approach might be useful as a low-cost, pre-screening of low abundance natural drugs, to identify potentially interesting unknown compounds (Lee et al., 2021). This concept of drug screening could be adapted easily to bigger pores like ClyA to expand to other drug targets like small proteins.

Sensing of proteins and protein dynamics

The success of nanopore sensing in nucleic acid sequencing has inspired its application for peptides and protein analysis (Alfaro et al., 2021; Restrepo-Pérez et al., 2018), in spite of the much larger complexity of amino acids compared to nucleobases. A ClyA pore mutant was for instance developed to trap the substrate binding domains 1 and 2 of an ATP-binding cassette importer in order to observe the conformational dynamics of the trapped protein with and without ligand (Van Meervelt et al., 2017) (Figure 3C). The trapped proteins, induced current fluctuations interpreted with conformational fluctuations associated to binding and unbinding of the ligand, which allowed for extraction of single-molecule protein kinetic features corresponding well to measurements with ensemble techniques as further shown for dihydrofolate reductase (Galenkamp et al., 2020). This method could facilitate access to a wealth of kinetic information with clinical importance. Because the observed protein kinetics is directly linked to the substrate concentration, the latter can be deduced from the observed conformational changes of the trapped protein. This metabolome analysis was used to accurately measure asparagine and glucose levels in sweat, blood, urine, and saliva as well as vitamin B1 in urine (Lucas et al., 2021a) without sample preparation (Galenkamp et al., 2018) and further proven with 8 other ligands (Zernia et al., 2020). The measured signal is reportedly influenced by interactions of the pore and the trapped protein, the dipole of the protein and its position inside of the nanopore. Kwak et al. adapted this approach to detect the neuraminidase activity of influenza virus in a timescale of minutes, which enables fast and early detection of infections (Kwak et al., 2020). For this purpose, an indirect readout was used: if present in the sample the neuraminidase cleaves off galactose from sialic acid derivatives, and the galactose level can be monitored by a D-galactose/D-glucose binding protein trapped in the ClyA nanopore which oscillates between open and closed state in a concentration dependent way. In turn, the detection limit of neuraminidases was 40- to 80-fold lower than electrochemical and ELISA immunocapture assays (Kwak et al., 2020).

The limited protein size range (up to 42 kDa (Zernia et al., 2020)) accessible to the ClyA pore shows the need for bigger biological nanopores, thus the significantly larger PlyAB pore was recently explored for similar purposes. An engineered version of PlyAB, designed to create an electroosmotic vortex allowing for easier protein entry and detection, was used to analyze two human serum proteins ranging from 67 to 81 kDa (Huang et al., 2020) (Figure 3D). Moreover, the same system was used to detect three hemoglobin variants in blood with near perfect accuracy and a sensitivity exceeding natural hemoglobin levels (Huang et al., 2021).

Another family of proteins whose dynamics has been investigated using biological nanopores is the motor proteins that are usually used to slow down DNA translocation in nanopore sequencing experiments (see also below). Using a MspA nanopore, the Gundlach lab has investigated the sequence dependent protein dynamics of polymerases and helicases associated with DNA backstepping and base-skipping mechanisms (Derrington et al., 2015; Laszlo et al., 2016).

Finally, protein-protein interactions can also be studied at single-molecule resolution using a biological nanopore (Figure 3E). Thakur and Movileanu proposed a method where a protein receptor of interest (e.g., RNase barnase, Bn in their case) is fused to an engineered FhuA ΔC/Δ4L nanopore with a flexible hexapeptide tether. A small negatively charged peptide (signal peptide) is further fused to the N-terminus of Bn, which interacts with the FhuA ΔC/Δ4L pore opening, providing a readout signal. When the fused protein of interest interacts with a protein binding partner the signal peptide is pulled out of the pore and the conductance increases, allowing to measure pulses related to the binding events and thus to the binding kinetics (Thakur and Movileanu, 2019a). The same group further applied their method as a selective sensor that is able to quantitatively detect the target proteins in serum (Thakur and Movileanu, 2019b). Multimeric pores with only one monomer carrying a fusion construct have been used by the Bayley lab to investigate

the dynamic process of protein phosphorylation and dephosphorylation (Harrington et al., 2019). Although these fusion-modified nanopores have the advantage of sensing the molecule outside of the nanopore which lifts the upper size limit of analytes that can be assessed, they lose the advantage of molecular resolution intrinsic to sensing inside of the nanopore lumen.

Sensing of peptides and unfolded proteins

Apart from the investigation of large, folded proteins, some studies deal with the seemingly easier task of sensing peptides and unfolded proteins exploiting the sensing capabilities of narrower pores. Chavis et al. showed that by electrophoretically trapping a negatively charged thiolate capped gold clusters ($Au_{25}(SG)_{18}$) of 2 nm in diameter in the vestibule of an α-HL pore, they can correlate the resistive pulses of five cationic peptides (5 to 13 amino acids long) to their mass (Chavis et al., 2017). A similar signal-mass relationship was later demonstrated using engineered FraC nanopores of different pore diameter, allowing identification of 19 different (4 to 22 amino acids) peptides with a 44 Da resolution (Huang et al., 2019). The high molecular resolution of biological nanopores for peptides was further demonstrated by Piguet et al. in aerolysin (Piguet et al., 2018).

Another study showed the differentiation in charge composition of highly cationic 12 amino acid-long peptides in a T7 DNA packing motor nanopore (Ji and Guo, 2019) and finally, a similar rationale was applied for the detection of post-translational modifications or mutations on short peptides with an engineered aerolysin pore. The pore was optimized to increase the analyte pore interactions, this increased interaction enhanced the residence time of the peptide inside the pore and by that enabled the detection of different phosphorylation states in a 9 amino acid fragment of tau (Li et al., 2020b) (Figure 3F). Prolonging the peptide residence time can also be achieved through bipolar peptides, where the peptide of interest is modified at both terminals with oppositely charged amino acids which facilitates entry but electrostatically hinders exit from the pore. This system was used to detect post-translational modifications (Restrepo-Pérez et al., 2019b) as well as chemical modifications (Restrepo-Pérez et al., 2019a) in short peptides with FraC nanopores. Another possibility is introducing rationally designed mutations at ideal positions for providing highest sensitivity for a given system, increasing for instance sensing accuracy for a short cationic peptide of HIV-1 Tat (Cao et al., 2019) using aerolysin pores, enabling the detection of different thioredoxin mutations with α-HL (Rodriguez-Larrea, 2021), or increasing capture and detection resolution of peptides in FraC (Lucas et al., 2021b).

Protein sequencing and fingerprinting

The majority of works on protein analysis have so far not been able to provide precise primary sequence information. *De novo* protein sequencing using nanopore sensing technologies is in fact the next big challenge after the recent successes with nucleic acid sequencing. However, the task appears much more arduous: first, 20 different amino acids need to be discriminated by current readout instead of 4 canonical bases. Assuming the same resolution of MspA for DNA sequencing, this would imply 16,000 possible quadromers one would need to classify (Laszlo et al., 2014), not considering the existence of numerous post-translational modifications that can decorate the native conformation of proteins in cellular conditions. Second, for accessing sequence information the protein of interest needs to be unfolded from its tertiary structure to be productively translocated within a nanopore. Third, the heterogeneous electrostatic nature of the polypeptide chain makes translocation by electrophoretic force challenging. Furthermore, the application of a universally applicable motor protein having the role to slow down, and control translocation as widely used for DNA sequencing appears to be more challenging with proteins. This is likely because of the nature of proteins, which unlike DNA are not meant to be sequentially read and copied, consequently there is a far greater abundance of DNA processive machinery than machinery that sequentially unfolds proteins. Nonetheless, the development of such a technique, which would allow for cheap and fast single-molecule quantitative proteome analysis of biological samples, is not too far-fetched when considering that nucleic acid sequencing has become a commercial reality in only 25 years. Some exciting results have recently emerged to address the above-mentioned issues in order to move the development of biological nanopore-based devices for single-molecule proteomics forward (Brinkerhoff et al., 2021; Yan et al., 2021).

Protein unfolding and subsequent translocation have been sparsely studied in solid-state nanopores (Restrepo-Pérez et al., 2017; Talaga and Li, 2009), the translocation of proteins as long as one thousand amino acids was demonstrated in 1 M GdmCl through aerolysin (Cressiot et al., 2015; Pastoriza-Gallego et al., 2011). The main issue related to unfolding is posed by the harsh chemical conditions needed, which can

be tolerated by DPhPC membranes at concentrations up to around 1.5 M for GdmCl (Cressiot et al., 2015; Yu et al., 2021) and at least 7.2 M for urea (Pastoriza-Gallego et al., 2007). SDS has not been shown to be compatible with these types of membranes although small amounts are likely to be tolerated. GdmCl unlike urea has the advantage that it does not lessen the conductivity of the electrolyte, and if compatible, SDS would be an interesting candidate because it would effectively charge the analyte. Their compatibility with biological nanopores varies from pore to pore but was demonstrated for the abovementioned conditions in aerolysin, MspA and α-HL for GdmCl (Cressiot et al., 2015; Yu et al., 2021) and in α-HL for urea (Pastoriza-Gallego et al., 2007). It remains to be seen if any of these agents can be successfully used with a multitude of proteins and nanopores.

Another strategy to unfold a protein relies on electrostatic pulling force as demonstrated for thioredoxin, which was captured with the help of an oligonucleotide attached to the C-terminus and gradually unfolded and translocated through an α-HL pore via a Brownian ratchet mechanism (Rodriguez-Larrea and Bayley, 2013; Simon et al., 1992) (Figure 3G). This unfolding through electrostatic pulling was also used to demonstrate the readout of protein expression levels through genetically encoded reporter proteins that are detectable with the commercial ONT sequencing platform, an approach that offers a significantly increased multiplexing potential (Cardozo et al., 2022). Subsequently, ClpX, the unfoldase of the ClpXP unfolding and degradation complex (Baker and Sauer, 2012), was adopted to pull folded proteins through α-HL pores. In this approach the target protein is C-terminally modified with an unfoldase recognition peptide to allow productive capturing and ATP-driven pulling (Nivala et al., 2013). Within a similar setting that included the full ClpXP complex to improve the number of successful translocations, different protein domains and mutational variants could be distinguished by looking at their unfolding signatures (Nivala et al., 2014). The main drawback of this approach is the need to include an *ad hoc* recognition peptide: although this can be easily engineered into expressed proteins, ideally it should be conjugated to the C-terminus of proteins posttranslationally to detect already expressed proteins.

The introduction of the ClpP exopeptidase starts addressing the even harsher problem of precisely identifying each single amino acid in a target protein. By cleaving residues one by one in the polypeptide chain, they can be subsequently detected by the nanopore (Asandei et al., 2020). The capability of sensing physicochemical differences of amino acids has recently been demonstrated when using aerolysin pores, which could discriminate 13 amino acid species by conjugating them to a 7 amino acid-long polyarginine to facilitate efficient capturing and optimizing the residence time within the pore (Ouldali et al., 2020). Considering that these engineered peptides are freely translocating through the pore, aerolysin demonstrates a remarkable and promising sensitivity for polypeptide chains.

A recent, impressive demonstration of nanopore bioengineering has taken us one step closer to actual protein sequencing with the design and expression of a multicomponent nanopore (in dark green in Figure 1D) that can thread and degrade proteins recognizing their C-terminus (Zhang et al., 2021a) (Figure 3H). This system can operate in two different modes: the thread-and-read mode where the folded analyte protein is unfolded and threaded through the pore and the cut-and-read mode in which the protein is degraded into peptides that subsequently translocate and are read through the nanopore. Remarkably, the unfolding process, which was shown for green fluorescence protein, does not influence the current signal. The problems that remain to be solved with this approach are the low resolution of the sensing module of the pore complex, and the consequential disability to sense the shortest of the cleaved peptides (Zhang et al., 2021a).

A second very recent step towards protein sequencing with an emphasis on reading accuracy has been shown by Brinkerhoff et al. who made use of a peptide-DNA hybrid molecule (26 amino acid-long linked to 80 nucleotides) and a DNA helicase for slowing the analyte. The DNA strand contains a helicase binding site and binds a complementary helicase stopper sequence. Upon analyte capture the peptide part translocates fully through the pore and the helicase stopper sequence is sheared off by the steric hindrance posed by the narrow MspA constriction. Now with the helicase stopper removed the helicase starts to pull the analyte back up in half-nucleotide steps, slowly pulling the peptide back up through the nanopore constriction. The helicase falls off once it reaches the end of the DNA part of the hybrid molecule which results in the complete analyte translocation. The analyte which has a maximum read length of 30 amino acids can be re-read many times reaching an identification accuracy of 100% and the ability to pick up single amino acid variations (Brinkerhoff et al., 2021). This was similarly demonstrated by Chen et al.

suggesting that stretching the analyte, thus limiting thermal motion would improve the resolution (Chen et al., 2021). Yan et al. demonstrated the same without rereading of the analyte employing a polymerase, and they suggested increasing the read length by extending the MspA pore mouth through protein engineering (Yan et al., 2021).

Despite the importance of sequence information, identification of the protein through fingerprinting would be already a valuable achievement which could deliver proteome information from a reference protein database. Ohayon et al. have indeed shown in a computational study that 99% of all proteins from the SwissProt database are identifiable by the detection of just three amino acids: lysine, cysteine, and methionine (Ohayon et al., 2019). Therefore, a method that would render these three markers readable to a nanopore would solve the issue of protein identification. Protein fingerprinting was demonstrated to be possible using mass spectrometry (Alfaro et al., 2021; Timp and Timp, 2020); however, despite its functionality, the technique exhibits significant drawbacks, which a nanopore-based framework would be able to solve.

OTHER REVIEW ARTICLES IN THE FIELD

Several reviews have discussed some of the topics of this review from different angles, and here we acknowledge their contribution on which we tried to expand. Majd et al. gave an exhaustive overview of the applications of biological nanopores beyond nanomedicine (Majd et al., 2010). Restrepo-Perez et al. discussed approaches to single-molecule protein sequencing in nanopores and beyond (Restrepo-Pérez et al., 2018). Recently, Alfaro et al. also reviewed this including a discussion on amino acid specific labeling techniques (Alfaro et al., 2021). Robertson & Reiner focused on protein and peptide sensing in biological and solid-state nanopores for various applications (Robertson and Reiner, 2018). Schmid and Dekker provided an updated piece on that topic (Schmid and Dekker, 2021). Chinappi & Cecconi gave an overview of the technical requirements for protein sequencing in nanopores and discussed the underlying transport phenomena and how to model them computationally (Chinappi and Cecconi, 2018). Callahan et al. discussed the current limits of proteomics and different approaches for next generation protein sequencing including nanopores (Callahan et al., 2020). Timp & Timp also discussed the new approaches in proteomics with a more thorough examination of solid-state nanopores (Timp and Timp, 2020). Hu et al. reviewed sequencing of proteins in biological nanopores and strategies to overcome the main challenges associated (Hu et al., 2020). Asandei et al. similarly debated the problems and solutions of protein sequencing, focusing on the α-HL nanopore (Asandei et al., 2020). In a recent review Robertson et al. discussed the chemistry of biological nanopores and its impact on the physical chemistry of nanopore sensing (Robertson et al., 2021). Finally, Cressiot et al. outlined the clinical importance of proteome sequencing with all levels of information beyond mere amino acids sequence and discussed protein sequencing and the main challenges of the technique for clinical applications (Cressiot et al., 2020).

CONCLUSIONS

It is remarkable that in only a few decades, we have been able to domesticate molecular machineries, which evolved to regulate cellular trafficking of entities spanning from single ions to large proteins, for the purpose of characterizing the same biological matter they are made of. Biological pores have found a prominent place in biotechnology with a major impact in the field of nanopore sensing, where their use has become ubiquitous with important applications in the field of genomics, proteomics, metabolomics, etc. They have stood out because their use is easy, cheap, and data can be collected in a matter of minutes through parallelization, minimal sample preparation and high throughput. Additionally, biological nanopores show extreme accuracy for a large spectrum of analytes and sense molecules individually which implicates many advantages over ensemble techniques. The possibility of miniaturization to pocket size (Deamer et al., 2016) devices is another stronghold that widens their application range. All these advantages have already been well-demonstrated in the commercialization by ONT of devices for DNA sequencing, which are widely employed and already have an edge over other DNA sequencing technologies despite being in their infancy.

The only drawbacks, which are still limiting their area of application as reviewed here, seem associated to our still incomplete knowledge of the physics underlying the translocation mechanism and to our imperfect ability to process and interpret current readout. Nonetheless, it is evident that the field's development is accelerated by the increasing rates of discoveries for applications in personalized medicine and single-molecule proteomics. Therefore, it is by no means unrealistic that the future progress in nanopore sensing,

including the use of engineered or fully synthetic pores, their merging with solid-state counterparts and full integration of artificial intelligence protocols, has the potential to shape the single-molecule sensing commodities of the future. Such as the sensing of amyloids in bodily fluids with the aim to follow the progression of neurodegenerative diseases (Houghtaling et al., 2018), the early and fast detection of viral infections like SARS-CoV-2 (Wang et al., 2020), bacterial infections (Moon et al., 2019) or cancers (Wang et al., 2011).

Although we have touched here specifically on biomedical related applications of biological nanopores, these same pores are finding promising ground in fields as diverse as detection of informational polymers for data storage (Cao et al., 2020; Ceze et al., 2019) and molecular tagging of physical objects (Doroschak et al., 2020). Even the analysis of chemicals in environmental probes could be well within reach. In conclusion, biological nanopores have proven to be highly versatile biological materials in both their native setting and in biotechnological applications; their ability to provide molecular-scale information about virtually any water-soluble entity proportionate to their pore lumen makes them appealing and effective tools across countless domains.

ACKNOWLEDGMENTS

We thank Aleksandra Radenovic, Sanjin Marion and Jared Houghtaling for several helpful discussions and review of the manuscript as well as Giovanni Maglia for providing the PDB file of the proteasome nanopore. This work was supported by the Swiss National Science Foundation (to M.D.P. and PR00P3_193090 to C.C.) and the Synapsis Foundation (2019-CDA02 to C.C.).

DECLARATION OF INTERESTS

The authors declare no competing interests.

REFERENCES

Aksimentiev, A., and Schulten, K. (2005). Imaging α-hemolysin with molecular dynamics: ionic conductance, osmotic permeability, and the electrostatic potential map. Biophys. J. *88*, 3745–3761. https://doi.org/10.1529/biophysj.104.058727.

Alfaro, J.A., Bohländer, P., Dai, M., Filius, M., Howard, C.J., van Kooten, X.F., Ohayon, S., Pomorski, A., Schmid, S., Aksimentiev, A., et al. (2021). The emerging landscape of single-molecule protein sequencing technologies. Nat. Methods *18*, 604–617. https://doi.org/10.1038/s41592-021-01143-1.

Asandei, A., Muccio, G.D., Schiopu, I., Mereuta, L., Dragomir, I.S., Chinappi, M., and Luchian, T. (2020). Nanopore-based protein sequencing using biopores: current achievements and open challenges. Small Methods *4*, 1900595. https://doi.org/10.1002/smtd.201900595.

Asandei, A., Schiopu, I., Chinappi, M., Seo, C.H., Park, Y., and Luchian, T. (2016). Electroosmotic trap against the electrophoretic force near a protein nanopore reveals peptide dynamics during capture and translocation. ACS Appl. Mater. Inter. *8*, 13166–13179. https://doi.org/10.1021/acsami.6b03697.

Awasthi, S., Sriboonpeng, P., Ying, C., Houghtaling, J., Shorubalko, I., Marion, S., Davis, S.J., Sola, L., Chiari, M., Radenovic, A., et al. (2020). Polymer coatings to minimize protein adsorption in solid-state nanopores. Small Methods *4*, 2000177. https://doi.org/10.1002/smtd.202000177.

Baker, T.A., and Sauer, R.T. (2012). ClpXP, an ATP-powered unfolding and protein-degradation machine. Biochim. Biophys. Acta BBA - Mol. Cell Res. 15–28. https://doi.org/10.1016/j.bbamcr.2011.06.007.

Bonome, E.L., Cecconi, F., and Chinappi, M. (2017). Electroosmotic flow through an α -hemolysin nanopore. Microfluid. Nanofluidics *21*, 96. https://doi.org/10.1007/s10404-017-1928-1.

Boukhet, M., Piguet, F., Ouldali, H., Pastoriza-Gallego, M., Pelta, J., and Oukhaled, A. (2016). Probing driving forces in aerolysin and α-hemolysin biological nanopores: electrophoresis versus electroosmosis. Nanoscale *8*, 18352–18359. https://doi.org/10.1039/C6NR06936C.

Brinkerhoff, H., Kang, A.S.W., Liu, J., Aksimentiev, A., and Dekker, C. (2021). Multiple rereads of single proteins at single–amino acid resolution using nanopores. Science *374*, 1509–1513. https://doi.org/10.1126/science.abl4381.

Butler, T.Z., Pavlenok, M., Derrington, I.M., Niederweis, M., and Gundlach, J.H. (2008). Single-molecule DNA detection with an engineered MspA protein nanopore. Proc. Natl. Acad. Sci. U S A *105*, 20647–20652. https://doi.org/10.1073/pnas.0807514106.

Callahan, N., Tullman, J., Kelman, Z., and Marino, J. (2020). Strategies for development of a next-generation protein sequencing platform. Trends Biochem. Sci. *45*, 76–89. https://doi.org/10.1016/j.tibs.2019.09.005.

Cao, C., Cirauqui, N., Marcaida, M.J., Buglakova, E., Duperrex, A., Radenovic, A., and Dal Peraro, M. (2019). Single-molecule sensing of peptides and nucleic acids by engineered aerolysin nanopores. Nat. Commun. *10*, 4918. https://doi.org/10.1038/s41467-019-12690-9.

Cao, C., Krapp, L.F., Ouahabi, A.A., König, N.F., Cirauqui, N., Radenovic, A., Lutz, J.-F., and Peraro, M.D. (2020). Aerolysin nanopores decode digital information stored in tailored macromolecular analytes. Sci. Adv. *6*, eabc2661. https://doi.org/10.1126/sciadv.abc2661.

Cao, C., Li, M.-Y., Cirauqui, N., Wang, Y.-Q., Dal Peraro, M., Tian, H., and Long, Y.-T. (2018). Mapping the sensing spots of aerolysin for single oligonucleotides analysis. Nat. Commun. *9*, 2823. https://doi.org/10.1038/s41467-018-05108-5.

Cardozo, N., Zhang, K., Doroschak, K., Nguyen, A., Siddiqui, Z., Bogard, N., Strauss, K., Ceze, L., and Nivala, J. (2022). Multiplexed direct detection of barcoded protein reporters on a nanopore array. Nat. Biotechnol. *40*, 42–46. https://doi.org/10.1038/s41587-021-01002-6.

Ceze, L., Nivala, J., and Strauss, K. (2019). Molecular digital data storage using DNA. Nat. Rev. Genet. *20*, 456–466. https://doi.org/10.1038/s41576-019-0125-3.

Chau, C.C., Hewitt, E.W., and Actis, P. (2021). The role of macromolecular crowding in single-entity electrochemistry: friend or foe? Curr. Opin. Electrochem. *25*, 100654. https://doi.org/10.1016/j.coelec.2020.100654.

Chau, C.C., Radford, S.E., Hewitt, E.W., and Actis, P. (2020). Macromolecular crowding enhances the detection of DNA and proteins by a solid-state nanopore. Nano Lett. *20*, 5553–5561. https://doi.org/10.1021/acs.nanolett.0c02246.

Chavis, A.E., Brady, K.T., Hatmaker, G.A., Angevine, C.E., Kothalawala, N., Dass, A., Robertson, J.W.F., and Reiner, J.E. (2017). Single molecule nanopore spectrometry for peptide detection. ACS Sens. *2*, 1319–1328. https://doi.org/10.1021/acssensors.7b00362.

Chen, X., Zhang, Y., Mohammadi Roozbahani, G., and Guan, X. (2019). Salt-Mediated nanopore

detection of ADAM-17. ACS Appl. Bio Mater. *2*, 504–509. https://doi.org/10.1021/acsabm.8b00689.

Chen, Z., Wang, Z., Xu, Y., Zhang, X., Tian, B., and Bai, J. (2021). Controlled movement of ssDNA conjugated peptide through Mycobacterium smegmatis porin A (MspA) nanopore by a helicase motor for peptide sequencing application. Chem. Sci. *12*, 15750–15756. https://doi.org/10.1039/D1SC04342K.

Cherf, G.M., Lieberman, K.R., Rashid, H., Lam, C.E., Karplus, K., and Akeson, M. (2012). Automated forward and reverse ratcheting of DNA in a nanopore at 5-Å precision. Nat. Biotechnol. *30*, 344–348. https://doi.org/10.1038/nbt.2147.

Chinappi, M., and Cecconi, F. (2018). Protein sequencing via nanopore based devices: a nanofluidics perspective. J. Phys. Condens. Matter *30*, 204002. https://doi.org/10.1088/1361-648X/aababe.

Cressiot, B., Bacri, L., and Pelta, J. (2020). The promise of nanopore technology: advances in the discrimination of protein sequences and chemical modifications. Small Methods *4*, 2000090. https://doi.org/10.1002/smtd.202000090.

Cressiot, B., Braselmann, E., Oukhaled, A., Elcock, A.H., Pelta, J., and Clark, P.L. (2015). Dynamics and energy contributions for transport of unfolded pertactin through a protein nanopore. ACS Nano *9*, 9050–9061. https://doi.org/10.1021/acsnano.5b03053.

Cressiot, B., Greive, S.J., Mojtabavi, M., Antson, A.A., and Wanunu, M. (2018). Thermostable virus portal proteins as reprogrammable adapters for solid-state nanopore sensors. Nat. Commun. *9*, 1–7. https://doi.org/10.1038/s41467-018-07116-x.

Crnković, A., Srnko, M., and Anderluh, G. (2021). Biological nanopores: engineering on demand. Life *11*, 27. https://doi.org/10.3390/life11010027.

Dal Peraro, M., and van der Goot, F.G. (2016). Pore-forming toxins: ancient, but never really out of fashion. Nat. Rev. Microbiol. *14*, 77–92. https://doi.org/10.1038/nrmicro.2015.3.

de Zoysa, R.S.S., Jayawardhana, D.A., Zhao, Q., Wang, D., Armstrong, D.W., and Guan, X. (2009). Slowing DNA translocation through nanopores using a solution containing organic salts. J. Phys. Chem. B *113*, 13332–13336. https://doi.org/10.1021/jp9040293.

Deamer, D., Akeson, M., and Branton, D. (2016). Three decades of nanopore sequencing. Nat. Biotechnol. *34*, 518–524. https://doi.org/10.1038/nbt.3423.

Derrington, I.M., Craig, J.M., Stava, E., Laszlo, A.H., Ross, B.C., Brinkerhoff, H., Nova, I.C., Doering, K., Tickman, B.I., Ronaghi, M., et al. (2015). Subangstrom single-molecule measurements of motor proteins using a nanopore. Nat. Biotechnol. *33*, 1073–1075. https://doi.org/10.1038/nbt.3357.

Díaz Carral, Á., Ostertag, M., and Fyta, M. (2021). Deep learning for nanopore ionic current blockades. J. Chem. Phys. *154*, 044111. https://doi.org/10.1063/5.0037938.

Doroschak, K., Zhang, K., Queen, M., Mandyam, A., Strauss, K., Ceze, L., and Nivala, J. (2020). Rapid and robust assembly and decoding of molecular tags with DNA-based nanopore signatures. Nat. Commun. *11*, 5454. https://doi.org/10.1038/s41467-020-19151-8.

Fahie, M.A., and Chen, M. (2015). Electrostatic interactions between OmpG nanopore and analyte protein surface can distinguish between glycosylated isoforms. J. Phys. Chem. B *119*, 10198–10206. https://doi.org/10.1021/acs.jpcb.5b06435.

Fahie, M.A., Yang, B., Mullis, M., Holden, M.A., and Chen, M. (2015). Selective detection of protein homologues in serum using an OmpG nanopore. Anal. Chem. *87*, 11143–11149. https://doi.org/10.1021/acs.analchem.5b03350.

Fennouri, A., List, J., Ducrey, J., Dupasquier, J., Sukyte, V., Mayer, S.F., Vargas, R.D., Pascual Fernandez, L., Bertani, F., Rodriguez Gonzalo, S., et al. (2021). Tuning the diameter, stability, and membrane affinity of peptide pores by DNA-programmed self-assembly. ACS Nano *15*, 11263–11275. https://doi.org/10.1021/acsnano.0c10311.

Fragasso, A., Schmid, S., and Dekker, C. (2020). Comparing current noise in biological and solid-state nanopores. ACS Nano *14*, 1338–1349. https://doi.org/10.1021/acsnano.9b09353.

Galenkamp, N.S., Biesemans, A., and Maglia, G. (2020). Directional conformer exchange in dihydrofolate reductase revealed by single-molecule nanopore recordings. Nat. Chem. *12*, 481–488. https://doi.org/10.1038/s41557-020-0437-0.

Galenkamp, N.S., Soskine, M., Hermans, J., Wloka, C., and Maglia, G. (2018). Direct electrical quantification of glucose and asparagine from bodily fluids using nanopores. Nat. Commun. *9*, 4085. https://doi.org/10.1038/s41467-018-06534-1.

Garalde, D.R., Snell, E.A., Jachimowicz, D., Sipos, B., Lloyd, J.H., Bruce, M., Pantic, N., Admassu, T., James, P., Warland, A., et al. (2018). Highly parallel direct RNA sequencing on an array of nanopores. Nat. Methods *15*, 201–206. https://doi.org/10.1038/nmeth.4577.

Goyal, P., Krasteva, P.V., Van Gerven, N., Gubellini, F., Van den Broeck, I., Troupiotis-Tsaïlaki, A., Jonckheere, W., Péhau-Arnaudet, G., Pinkner, J.S., Chapman, M.R., et al. (2014). Structural and mechanistic insights into the bacterial amyloid secretion channel CsgG. Nature *516*, 250–253. https://doi.org/10.1038/nature13768.

Hall, A.R., Scott, A., Rotem, D., Mehta, K.K., Bayley, H., and Dekker, C. (2010). Hybrid pore formation by directed insertion of α-haemolysin into solid-state nanopores. Nat. Nanotechnol. *5*, 874–877. https://doi.org/10.1038/nnano.2010.237.

Hall, J.E. (1975). Access resistance of a small circular pore. J. Gen. Physiol. *66*, 531–532. https://doi.org/10.1085/jgp.66.4.531.

Hanke, W., and Schlue, W.-R. (1993). Planar Lipid Bilayers Methods and Applications (Academic Press).

Harrington, L., Alexander, L.T., Knapp, S., and Bayley, H. (2019). Single-molecule protein phosphorylation and dephosphorylation by nanopore enzymology. ACS Nano *13*, 633–641. https://doi.org/10.1021/acsnano.8b07697.

Houghtaling, J. (2019). Label-Free Characterization of Single Proteins Using Synthetic Nanopores (University of Michigan).

Houghtaling, J., List, J., and Mayer, M. (2018). Nanopore-based, rapid characterization of individual amyloid particles in solution: concepts, challenges, and prospects. Small *14*, 1802412. https://doi.org/10.1002/smll.201802412.

Hu, Z.-L., Huo, M.-Z., Ying, Y.-L., and Long, Y.-T. (2020). Biological nanopore approach for single-molecule protein sequencing. Angew. Chem. Int. Ed. *60*, 14738–14749. https://doi.org/10.1002/anie.202013462.

Hu, Z.-L., Li, M.-Y., Liu, S.-C., Ying, Y.-L., and Long, Y.-T. (2019). A lithium-ion-active aerolysin nanopore for effectively trapping long single-stranded DNA. Chem. Sci. *10*, 354–358. https://doi.org/10.1039/C8SC03927E.

Huang, G., Versloot, R.C.A., and Maglia, G. (2021). Detection of single amino acid differences in haemoglobin from blood samples using a nanopore. Preprint at chemRxiv. https://doi.org/10.26434/chemrxiv-2021-7gb4h.

Huang, G., Voet, A., and Maglia, G. (2019). FraC nanopores with adjustable diameter identify the mass of opposite-charge peptides with 44 dalton resolution. Nat. Commun. *10*, 1–10. https://doi.org/10.1038/s41467-019-08761-6.

Huang, G., Willems, K., Bartelds, M., van Dorpe, P., Soskine, M., and Maglia, G. (2020). Electro-osmotic vortices promote the capture of folded proteins by PlyAB nanopores. Nano Lett. *20*, 3819–3827. https://doi.org/10.1021/acs.nanolett.0c00877.

Huang, G., Willems, K., Soskine, M., Wloka, C., and Maglia, G. (2017). Electro-osmotic capture and ionic discrimination of peptide and protein biomarkers with FraC nanopores. Nat. Commun. *8*, 935. https://doi.org/10.1038/s41467-017-01006-4.

Ivica, J., Williamson, P.T.F., and de Planque, M.R.R. (2017). Salt gradient modulation of MicroRNA translocation through a biological nanopore. Anal. Chem. *89*, 8822–8829. https://doi.org/10.1021/acs.analchem.7b01246.

Jarockyte, G., Karabanovas, V., Rotomskis, R., and Mobasheri, A. (2020). Multiplexed nanobiosensors: current trends in early diagnostics. Sensors *20*, 6890. https://doi.org/10.3390/s20236890.

Ji, Z., and Guo, P. (2019). Channel from bacterial virus T7 DNA packaging motor for the differentiation of peptides composed of a mixture of acidic and basic amino acids. Biomaterials *214*, 119222. https://doi.org/10.1016/j.biomaterials.2019.119222.

Johnson, B.B., and Heuck, A.P. (2014). Perfringolysin O structure and mechanism of pore formation as a paradigm for cholesterol-dependent cytolysins. Subcell. Biochem. *80*, 63–81. https://doi.org/10.1007/978-94-017-8881-6_5.

Johnson, R.P., Fleming, A.M., Perera, R.T., Burrows, C.J., and White, H.S. (2017). Dynamics of a DNA mismatch site held in confinement discriminate epigenetic modifications of cytosine. J. Am. Chem. Soc. *139*, 2750–2756. https://doi.org/10.1021/jacs.6b12284.

Kang, X., Alibakhshi, M.A., and Wanunu, M. (2019). One-pot species release and nanopore detection in a voltage-stable lipid bilayer platform. Nano Lett. *19*, 9145–9153. https://doi.org/10.1021/acs.nanolett.9b04446.

Kang, X., Cheley, S., Rice-Ficht, A.C., and Bayley, H. (2007). A storable encapsulated bilayer chip containing a single protein nanopore. J. Am. Chem. Soc. *129*, 4701–4705. https://doi.org/10.1021/ja068654g.

Kasianowicz, J.J., Brandin, E., Branton, D., and Deamer, D.W. (1996). Characterization of individual polynucleotide molecules using a membrane channel. Proc. Natl. Acad. Sci. *93*, 13770–13773. https://doi.org/10.1073/pnas.93.24.13770.

Keller, M.W., Rambo-Martin, B.L., Wilson, M.M., Ridenour, C.A., Shepard, S.S., Stark, T.J., Neuhaus, E.B., Dugan, V.G., Wentworth, D.E., and Barnes, J.R. (2018). Direct RNA sequencing of the coding complete influenza A virus genome. Sci. Rep. *8*, 14408. https://doi.org/10.1038/s41598-018-32615-8.

Kim, D., Lee, J.-Y., Yang, J.-S., Kim, J.W., Kim, V.N., and Chang, H. (2020). The architecture of SARS-CoV-2 transcriptome. Cell *181*, 914–921.e10. https://doi.org/10.1016/j.cell.2020.04.011.

Kowalczyk, S.W., Grosberg, A.Y., Rabin, Y., and Dekker, C. (2011). Modeling the conductance and DNA blockade of solid-state nanopores. Nanotechnology *22*, 315101. https://doi.org/10.1088/0957-4484/22/31/315101.

Kowalczyk, S.W., Wells, D.B., Aksimentiev, A., and Dekker, C. (2012). Slowing down DNA translocation through a nanopore in lithium chloride. Nano Lett. *12*, 1038–1044. https://doi.org/10.1021/nl204273h.

Kutzner, C., Grubmüller, H., de Groot, B.L., and Zachariae, U. (2011). Computational electrophysiology: the molecular dynamics of ion channel permeation and selectivity in atomistic detail. Biophys. J. *101*, 809–817. https://doi.org/10.1016/j.bpj.2011.06.010.

Kwak, D.-K., Kim, J.-S., Lee, M.-K., Ryu, K.-S., and Chi, S.-W. (2020). Probing the neuraminidase activity of influenza virus using a cytolysin A protein nanopore. Anal. Chem. *92*, 14303–14308. https://doi.org/10.1021/acs.analchem.0c03399.

Lan, W.-J., Holden, D.A., Liu, J., and White, H.S. (2011). Pressure-driven nanoparticle transport across glass membranes containing a conical-shaped nanopore. J. Phys. Chem. C *115*, 18445–18452. https://doi.org/10.1021/jp204839j.

Larimi, M.G., Mayse, L.A., and Movileanu, L. (2019). Interactions of a polypeptide with a protein nanopore under crowding conditions. ACS Nano *13*, 4469–4477. https://doi.org/10.1021/acsnano.9b00008.

Laszlo, A.H., Derrington, I.M., Brinkerhoff, H., Langford, K.W., Nova, I.C., Samson, J.M., Bartlett, J.J., Pavlenok, M., and Gundlach, J.H. (2013). Detection and mapping of 5-methylcytosine and 5-hydroxymethylcytosine with nanopore MspA. Proc. Natl. Acad. Sci. *110*, 18904–18909. https://doi.org/10.1073/pnas.1310240110.

Laszlo, A.H., Derrington, I.M., and Gundlach, J.H. (2016). MspA nanopore as a single-molecule tool: from sequencing to SPRNT. Methods Single molecule probing by fluorescence force Detect. *105*, 75–89. https://doi.org/10.1016/j.ymeth.2016.03.026.

Laszlo, A.H., Derrington, I.M., Ross, B.C., Brinkerhoff, H., Adey, A., Nova, I.C., Craig, J.M., Langford, K.W., Samson, J.M., Daza, R., et al. (2014). Decoding long nanopore sequencing reads of natural DNA. Nat. Biotechnol. *32*, 829–833. https://doi.org/10.1038/nbt.2950.

Lee, D.-H., Oh, S., Lim, K., Lee, B., Yi, G.-S., Kim, Y.-R., Kim, K.-B., Lee, C.-K., Chi, S.-W., and Lee, M.-K. (2021). Tertiary RNA folding-targeted drug screening strategy using a protein nanopore. Anal. Chem. *93*, 2811–2819. https://doi.org/10.1021/acs.analchem.0c03941.

Li, M.-Y., Ying, Y.-L., Li, S., Wang, Y.-Q., Wu, X.-Y., and Long, Y.-T. (2020a). Unveiling the heterogenous dephosphorylation of DNA using an aerolysin nanopore. ACS Nano *14*, 12571–12578. https://doi.org/10.1021/acsnano.0c03215.

Li, S., Wu, X.-Y., Li, M.-Y., Liu, S.-C., Ying, Y.-L., and Long, Y.-T. (2020b). T232K/K238Q aerolysin nanopore for mapping adjacent phosphorylation sites of a single tau peptide. Small Methods *4*, 2000014. https://doi.org/10.1002/smtd.202000014.

Lieberman, K.R., Cherf, G.M., Doody, M.J., Olasagasti, F., Kolodji, Y., and Akeson, M. (2010). Processive replication of single DNA molecules in a nanopore catalyzed by phi29 DNA polymerase. J. Am. Chem. Soc. *132*, 17961–17972. https://doi.org/10.1021/ja1087612.

Liu, P., and Kawano, R. (2020). Recognition of single-point mutation using a biological nanopore. Small Methods *4*, 2000101. https://doi.org/10.1002/smtd.202000101.

Liu, Y., Wang, K., Wang, Y., Wang, L., Yan, S., Du, X., Zhang, P., Chen, H.-Y., and Huang, S. (2022). Machine learning assisted simultaneous structural profiling of differently charged proteins in a Mycobacterium smegmatis porin A (MspA) electroosmotic trap. J. Am. Chem. Soc. *144*, 757–768. https://doi.org/10.1021/jacs.1c09259.

Lucas, F.L.R., Piso, T.R.C., van der Heide, N.J., Galenkamp, N.S., Hermans, J., Wloka, C., and Maglia, G. (2021a). Automated electrical quantification of vitamin B1 in a bodily fluid using an engineered nanopore-sensor. Angew. Chem. Int. Ed. *60*, 22849–22855. https://doi.org/10.1002/anie.202107807.

Lucas, F.L.R., Sarthak, K., Lenting, E.M., Coltan, D., van der Heide, N.J., Versloot, R.C.A., Aksimentiev, A., and Maglia, G. (2021b). The manipulation of the internal hydrophobicity of FraC nanopores augments peptide capture and recognition. ACS Nano *15*, 9600–9613. https://doi.org/10.1021/acsnano.0c09958.

Maglia, G., Restrepo, M.R., Mikhailova, E., and Bayley, H. (2008). Enhanced translocation of single DNA molecules through -hemolysin nanopores by manipulation of internal charge. Proc. Natl. Acad. Sci. *105*, 19720–19725. https://doi.org/10.1073/pnas.0808296105.

Majd, S., Yusko, E.C., Billeh, Y.N., Macrae, M.X., Yang, J., and Mayer, M. (2010). Applications of biological pores in nanomedicine, sensing, and nanoelectronics. Curr. Opin. Biotechnol. *21*, 439–476. https://doi.org/10.1016/j.copbio.2010.05.002.

Malmstadt, N., Jeon, T.-J., and Schmidt, J.J. (2008). Long-lived planar lipid bilayer membranes anchored to an in situ polymerized hydrogel. Adv. Mater. *20*, 84–89. https://doi.org/10.1002/adma.200700810.

Manrao, E.A., Derrington, I.M., Laszlo, A.H., Langford, K.W., Hopper, M.K., Gillgren, N., Pavlenok, M., Niederweis, M., and Gundlach, J.H. (2012). Reading DNA at single-nucleotide resolution with a mutant MspA nanopore and phi29 DNA polymerase. Nat. Biotechnol. *30*, 349–353. https://doi.org/10.1038/nbt.2171.

Mathé, J., Aksimentiev, A., Nelson, D.R., Schulten, K., and Meller, A. (2005). Orientation discrimination of single-stranded DNA inside the α-hemolysin membrane channel. Proc. Natl. Acad. Sci. *102*, 12377–12382. https://doi.org/10.1073/pnas.0502947102.

Misiunas, K., Ermann, N., and Keyser, U.F. (2018). QuipuNet: convolutional neural network for single-molecule nanopore sensing. Nano Lett. *18*, 4040–4045. https://doi.org/10.1021/acs.nanolett.8b01709.

Modi, N., Singh, P.R., Mahendran, K.R., Schulz, R., Winterhalter, M., and Kleinekathöfer, U. (2011). Probing the transport of ionic liquids in aqueous solution through nanopores. J. Phys. Chem. Lett. *2*, 2331–2336. https://doi.org/10.1021/jz201006b.

Moon, J., Kim, N., Kim, T.-J., Jun, J.-S., Lee, H.S., Shin, H.-R., Lee, S.-T., Jung, K.-H., Park, K.-I., Jung, K.-Y., et al. (2019). Rapid diagnosis of bacterial meningitis by nanopore 16S amplicon sequencing: a pilot study. Int. J. Med. Microbiol. *309*, 151338. https://doi.org/10.1016/j.ijmm.2019.151338.

Ni, P., Huang, N., Zhang, Z., Wang, D.-P., Liang, F., Miao, Y., Xiao, C.-L., Luo, F., and Wang, J. (2019). DeepSignal: detecting DNA methylation state from Nanopore sequencing reads using deep-learning. Bioinformatics *35*, 4586–4595. https://doi.org/10.1093/bioinformatics/btz276.

Niedzwiecki, D.J., Mohammad, M.M., and Movileanu, L. (2012). Inspection of the engineered FhuA ΔC/Δ4L protein nanopore by polymer exclusion. Biophys. J. *103*, 2115–2124. https://doi.org/10.1016/j.bpj.2012.10.008.

Nivala, J., Marks, D.B., and Akeson, M. (2013). Unfoldase-mediated protein translocation through an α-hemolysin nanopore. Nat. Biotechnol. *31*, 247–250. https://doi.org/10.1038/nbt.2503.

Nivala, J., Mulroney, L., Li, G., Schreiber, J., and Akeson, M. (2014). Discrimination among protein variants using an unfoldase-coupled nanopore. ACS Nano *8*, 12365–12375. https://doi.org/10.1021/nn5049987.

Oh, S., Lee, M.-K., and Chi, S.-W. (2019). Single-molecule-based detection of conserved influenza

A virus RNA promoter using a protein nanopore. ACS Sens. *4*, 2849–2853. https://doi.org/10.1021/acssensors.9b01558.

Ohayon, S., Girsault, A., Nasser, M., Shen-Orr, S., and Meller, A. (2019). Simulation of single-protein nanopore sensing shows feasibility for whole-proteome identification. PLoS Comput. Biol. *15*, e1007067. https://doi.org/10.1371/journal.pcbi.1007067.

Ouldali, H., Sarthak, K., Ensslen, T., Piguet, F., Manivet, P., Pelta, J., Behrends, J.C., Aksimentiev, A., and Oukhaled, A. (2020). Electrical recognition of the twenty proteinogenic amino acids using an aerolysin nanopore. Nat. Biotechnol. *38*, 176–181. https://doi.org/10.1038/s41587-019-0345-2.

Pastoriza-Gallego, M., Oukhaled, G., Mathé, J., Thiebot, B., Betton, J.-M., Auvray, L., and Pelta, J. (2007). Urea denaturation of α-hemolysin pore inserted in planar lipid bilayer detected by single nanopore recording: loss of structural asymmetry. FEBS Lett. *581*, 3371–3376. https://doi.org/10.1016/j.febslet.2007.06.036.

Pastoriza-Gallego, M., Rabah, L., Gibrat, G., Thiebot, B., van der Goot, F.G., Auvray, L., Betton, J.-M., and Pelta, J. (2011). Dynamics of unfolded protein transport through an aerolysin pore. J. Am. Chem. Soc. *133*, 2923–2931. https://doi.org/10.1021/ja1073245.

Payet, L., Martinho, M., Merstorf, C., Pastoriza-Gallego, M., Pelta, J., Viasnoff, V., Auvray, L., Muthukumar, M., and Mathé, J. (2015). Temperature effect on ionic current and ssDNA transport through nanopores. Biophys. J. *109*, 1600–1607. https://doi.org/10.1016/j.bpj.2015.08.043.

Pennisi, E. (2016). Pocket DNA sequencers make real-time diagnostics a reality. Science *351*, 800–801. https://doi.org/10.1126/science.351.6275.800.

Piguet, F., Ouldali, H., Pastoriza-Gallego, M., Manivet, P., Pelta, J., and Oukhaled, A. (2018). Identification of single amino acid differences in uniformly charged homopolymeric peptides with aerolysin nanopore. Nat. Commun. *9*, 966. https://doi.org/10.1038/s41467-018-03418-2.

Plesa, C., and Dekker, C. (2015). Data analysis methods for solid-state nanopores. Nanotechnology *26*, 084003. https://doi.org/10.1088/0957-4484/26/8/084003.

Purnell, R.F., and Schmidt, J.J. (2009). Discrimination of single base substitutions in a DNA strand immobilized in a biological nanopore. ACS Nano *3*, 2533–2538. https://doi.org/10.1021/nn900441x.

Restrepo-Pérez, L., Huang, G., Bohländer, P.R., Worp, N., Eelkema, R., Maglia, G., Joo, C., and Dekker, C. (2019a). Resolving chemical modifications to a single amino acid within a peptide using a biological nanopore. ACS Nano *13*, 13668–13676. https://doi.org/10.1021/acsnano.9b05156.

Restrepo-Pérez, L., John, S., Aksimentiev, A., Joo, C., and Dekker, C. (2017). SDS-assisted protein transport through solid-state nanopores. Nanoscale *9*, 11685–11693. https://doi.org/10.1039/C7NR02450A.

Restrepo-Pérez, L., Joo, C., and Dekker, C. (2018). Paving the way to single-molecule protein sequencing. Nat. Nanotechnol. *13*, 786–796. https://doi.org/10.1038/s41565-018-0236-6.

Restrepo-Pérez, L., Wong, C.H., Maglia, G., Dekker, C., and Joo, C. (2019b). Label-free detection of post-translational modifications with a nanopore. Nano Lett. *19*, 7957–7964. https://doi.org/10.1021/acs.nanolett.9b03134.

Robertson, J.W.F., Ghimire, M.L., and Reiner, J.E. (2021). Nanopore sensing: a physical-chemical approach. Biochim. Biophys. Acta BBA - Biomembr. *1863*, 183644. https://doi.org/10.1016/j.bbamem.2021.183644.

Robertson, J.W.F., Kasianowicz, J.J., and Banerjee, S. (2012). Analytical approaches for studying transporters, channels and porins. Chem. Rev. *112*, 6227–6249. https://doi.org/10.1021/cr300317z.

Robertson, J.W.F., and Reiner, J.E. (2018). The utility of nanopore technology for protein and peptide sensing. Proteomics *18*, 1800026. https://doi.org/10.1002/pmic.201800026.

Rodriguez-Larrea, D. (2021). Single-aminoacid discrimination in proteins with homogeneous nanopore sensors and neural networks. Biosens. Bioelectron. *180*, 113108. https://doi.org/10.1016/j.bios.2021.113108.

Rodriguez-Larrea, D., and Bayley, H. (2013). Multistep protein unfolding during nanopore translocation. Nat. Nanotechnol. *8*, 288–295. https://doi.org/10.1038/nnano.2013.22.

Rosen, C.B., Rodriguez-Larrea, D., and Bayley, H. (2014). Single-molecule site-specific detection of protein phosphorylation with a nanopore. Nat. Biotechnol. *32*, 179–181. https://doi.org/10.1038/nbt.2799.

Schmid, S., and Dekker, C. (2021). Nanopores: a versatile tool to study protein dynamics. Essays Biochem. *65*, 93–107. https://doi.org/10.1042/EBC20200020.

Simon, S.M., Peskin, C.S., and Oster, G.F. (1992). What drives the translocation of proteins? Proc. Natl. Acad. Sci. *89*, 3770–3774. https://doi.org/10.1073/pnas.89.9.3770.

Smith, M.A., Ersavas, T., Ferguson, J.M., Liu, H., Lucas, M.C., Begik, O., Bojarski, L., Barton, K., and Novoa, E.M. (2020). Molecular barcoding of native RNAs using nanopore sequencing and deep learning. Genome Res. *30*, 1345–1353. https://doi.org/10.1101/gr.260836.120.

Song, L., Hobaugh, M.R., Shustak, C., Cheley, S., Bayley, H., and Gouaux, J.E. (1996). Structure of staphylococcal α-hemolysin, a heptameric transmembrane pore. Science *274*, 1859–1865. https://doi.org/10.1126/science.274.5294.1859.

Soskine, M., Biesemans, A., De Maeyer, M., and Maglia, G. (2013). Tuning the size and properties of ClyA nanopores assisted by directed evolution. J. Am. Chem. Soc. *135*, 13456–13463. https://doi.org/10.1021/ja4053398.

Stoddart, D., Heron, A.J., Mikhailova, E., Maglia, G., and Bayley, H. (2009). Single-nucleotide discrimination in immobilized DNA oligonucleotides with a biological nanopore. Proc. Natl. Acad. Sci. *106*, 7702–7707. https://doi.org/10.1073/pnas.0901054106.

Talaga, D.S., and Li, J. (2009). Single-molecule protein unfolding in solid state nanopores. J. Am. Chem. Soc. *131*, 9287–9297. https://doi.org/10.1021/ja901088b.

Taniguchi, M., Minami, S., Ono, C., Hamajima, R., Morimura, A., Hamaguchi, S., Akeda, Y., Kanai, Y., Kobayashi, T., Kamitani, W., et al. (2021). Combining machine learning and nanopore construction creates an artificial intelligence nanopore for coronavirus detection. Nat. Commun. *12*, 3726. https://doi.org/10.1038/s41467-021-24001-2.

Teng, H., Cao, M.D., Hall, M.B., Duarte, T., Wang, S., and Coin, L.J.M. (2018). Chiron: translating nanopore raw signal directly into nucleotide sequence using deep learning. GigaScience *7*, giy037. https://doi.org/10.1093/gigascience/giy037.

Thakur, A.K., and Movileanu, L. (2019a). Real-time measurement of protein–protein interactions at single-molecule resolution using a biological nanopore. Nat. Biotechnol. *37*, 96–101. https://doi.org/10.1038/nbt.4316.

Thakur, A.K., and Movileanu, L. (2019b). Single-molecule protein detection in a biofluid using a quantitative nanopore sensor. ACS Sens. *4*, 2320–2326. https://doi.org/10.1021/acssensors.9b00848.

Timp, W., and Timp, G. (2020). Beyond mass spectrometry, the next step in proteomics. Sci. Adv. *6*, eaax8978. https://doi.org/10.1126/sciadv.aax8978.

Van der Verren, S.E., Van Gerven, N., Jonckheere, W., Hambley, R., Singh, P., Kilgour, J., Jordan, M., Wallace, E.J., Jayasinghe, L., and Remaut, H. (2020). A dual-constriction biological nanopore resolves homonucleotide sequences with high fidelity. Nat. Biotechnol. *38*, 1415–1420. https://doi.org/10.1038/s41587-020-0570-8.

Van Meervelt, V., Soskine, M., Singh, S., Schuurman-Wolters, G.K., Wijma, H.J., Poolman, B., and Maglia, G. (2017). Real-time conformational changes and controlled orientation of native proteins inside a protein nanoreactor. J. Am. Chem. Soc. *139*, 18640–18646. https://doi.org/10.1021/jacs.7b10106.

Viehweger, A., Krautwurst, S., Lamkiewicz, K., Madhugiri, R., Ziebuhr, J., Hölzer, M., and Marz, M. (2019). Direct RNA nanopore sequencing of full-length coronavirus genomes provides novel insights into structural variants and enables modification analysis. Genome Res. *29*, 1545–1554. https://doi.org/10.1101/gr.247064.118.

Wang, H.-Y., Li, Y., Qin, L.-X., Heyman, A., Shoseyov, O., Willner, I., Long, Y.-T., and Tian, H. (2013a). Single-molecule DNA detection using a novel SP1 protein nanopore. Chem. Commun. *49*, 1741–1743. https://doi.org/10.1039/C3CC38939A.

Wang, M., Fu, A., Hu, B., Tong, Y., Liu, R., Liu, Z., Gu, J., Xiang, B., Liu, J., Jiang, W., et al. (2020). Nanopore targeted sequencing for the accurate and comprehensive detection of SARS-CoV-2 and other respiratory viruses. Small *16*, 2002169. https://doi.org/10.1002/smll.202002169.

Wang, S., Haque, F., Rychahou, P.G., Evers, B.M., and Guo, P. (2013b). Engineered nanopore of phi 29 DNA-packaging motor for real-time detection of single colon cancer specific antibody in serum. ACS Nano *7*, 9814–9822. https://doi.org/10.1021/nn404435v.

Wang, Y., Zheng, D., Tan, Q., Wang, M.X., and Gu, L.-Q. (2011). Nanopore-based detection of circulating microRNAs in lung cancer patients. Nat. Nanotechnol. *6*, 668–674. https://doi.org/10.1038/nnano.2011.147.

Wang, Y., Zhang, Y., Guo, Y., and Kang, X. (2017a). Fast and precise detection of DNA methylation with tetramethylammonium-filled nanopore. Sci. Rep. *7*, 183. https://doi.org/10.1038/s41598-017-00317-2.

Wang, Y., Tian, K., Du, X., Shi, R.-C., and Gu, L.-Q. (2017b). Remote activation of a nanopore for high-performance genetic detection using a pH taxis-mimicking mechanism. Anal. Chem. *89*, 13039–13043. https://doi.org/10.1021/acs.analchem.7b03979.

Wanunu, M., Morrison, W., Rabin, Y., Grosberg, A.Y., and Meller, A. (2010). Electrostatic focusing of unlabelled DNA into nanoscale pores using a salt gradient. Nat. Nanotechnol. *5*, 160–165. https://doi.org/10.1038/nnano.2009.379.

Willems, K., Ruić, D., Biesemans, A., Galenkamp, N.S., Van Dorpe, P., and Maglia, G. (2019). Engineering and modeling the electrophoretic trapping of a single protein inside a nanopore. ACS Nano *13*, 9980–9992. https://doi.org/10.1021/acsnano.8b09137.

Wilson, J., Sarthak, K., Si, W., Gao, L., and Aksimentiev, A. (2019). Rapid and accurate determination of nanopore ionic current using a steric exclusion model. ACS Sens. *4*, 634–644. https://doi.org/10.1021/acssensors.8b01375.

Wloka, C., Mutter, N.L., Soskine, M., and Maglia, G. (2016). Alpha-helical fragaceatoxin C nanopore engineered for double-stranded and single-stranded nucleic acid analysis. Angew. Chem. Int. Ed. *55*, 12494–12498. https://doi.org/10.1002/anie.201606742.

Woringer, M., Izeddin, I., Favard, C., and Berry, H. (2020). Anomalous subdiffusion in living cells: bridging the gap between experiments and realistic models through collaborative challenges. Front. Phys. *8*, 134. https://doi.org/10.3389/fphy.2020.00134.

Wu, H.-C., Astier, Y., Maglia, G., Mikhailova, E., and Bayley, H. (2007). Protein nanopores with covalently attached molecular adapters. J. Am. Chem. Soc. *129*, 16142–16148. https://doi.org/10.1021/ja0761840.

Xi, D., Li, Z., Liu, L., Ai, S., and Zhang, S. (2018). Ultrasensitive detection of cancer cells combining enzymatic signal amplification with an aerolysin nanopore. Anal. Chem. *90*, 1029–1034. https://doi.org/10.1021/acs.analchem.7b04584.

Xu, C., Lu, P., Gamal El-Din, T.M., Pei, X.Y., Johnson, M.C., Uyeda, A., Bick, M.J., Xu, Q., Jiang, D., Bai, H., et al. (2020). Computational design of transmembrane pores. Nature *585*, 129–134. https://doi.org/10.1038/s41586-020-2646-5.

Xue, L., Yamazaki, H., Ren, R., Wanunu, M., Ivanov, A.P., and Edel, J.B. (2020). Solid-state nanopore sensors. Nat. Rev. Mater. *5*, 931–951. https://doi.org/10.1038/s41578-020-0229-6.

Yan, S., Zhang, J., Wang, Y., Guo, W., Zhang, S., Liu, Y., Cao, J., Wang, Y., Wang, L., Ma, F., et al. (2021). Single molecule ratcheting motion of peptides in a Mycobacterium smegmatis porin A (MspA) nanopore. Nano Lett. *21*, 6703–6710. https://doi.org/10.1021/acs.nanolett.1c02371.

Yao, F., Peng, X., Su, Z., Tian, L., Guo, Y., and Kang, X. (2020). Crowding-induced DNA translocation through a protein nanopore. Anal. Chem. *92*, 3827–3833. https://doi.org/10.1021/acs.analchem.9b05249.

Yu, L., Kang, X., Alibakhshi, M.A., Pavlenok, M., Niederweis, M., and Wanunu, M. (2021). Stable polymer bilayers for protein channel recordings at high guanidinium chloride concentrations. Biophys. J. *120*, 1537–1541. https://doi.org/10.1016/j.bpj.2021.02.019.

Yusko, E.C., Bruhn, B.R., Eggenberger, O.M., Houghtaling, J., Rollings, R.C., Walsh, N.C., Nandivada, S., Pindrus, M., Hall, A.R., Sept, D., et al. (2017). Real-time shape approximation and fingerprinting of single proteins using a nanopore. Nat. Nanotechnol. *12*, 360–367. https://doi.org/10.1038/nnano.2016.267.

Yusko, E.C., Johnson, J.M., Majd, S., Prangkio, P., Rollings, R.C., Li, J., Yang, J., and Mayer, M. (2011). Controlling protein translocation through nanopores with bio-inspired fluid walls. Nat. Nanotechnol. *6*, 253–260. https://doi.org/10.1038/nnano.2011.12.

Zernia, S., van der Heide, N.J., Galenkamp, N.S., Gouridis, G., and Maglia, G. (2020). Current blockades of proteins inside nanopores for real-time metabolome analysis. ACS Nano *14*, 2296–2307. https://doi.org/10.1021/acsnano.9b09434.

Zhang, S., Huang, G., Versloot, R.C.A., Bruininks, B.M.H., de Souza, P.C.T., Marrink, S.-J., and Maglia, G. (2021a). Bottom-up fabrication of a proteasome–nanopore that unravels and processes single proteins. Nat. Chem. *13*, 1192–1199. https://doi.org/10.1038/s41557-021-00824-w.

Zhang, X., Dou, L., Zhang, M., Wang, Y., Jiang, X., Li, X., Wei, L., Chen, Y., Zhou, C., and Geng, J. (2021b). Real-time sensing of neurotransmitters by functionalized nanopores embedded in a single live cell. Mol. Biomed. *2*, 6. https://doi.org/10.1186/s43556-021-00026-3.

Zhang, Z., Wang, X., Wei, X., Zheng, S.W., Lenhart, B.J., Xu, P., Li, J., Pan, J., Albrecht, H., and Liu, C. (2021c). Multiplex quantitative detection of SARS-CoV-2 specific IgG and IgM antibodies based on DNA-assisted nanopore sensing. Biosens. Bioelectron. *181*, 113134. https://doi.org/10.1016/j.bios.2021.113134.

Zhou, Z., Ji, Z., Wang, S., Haque, F., and Guo, P. (2016). Oriented single directional insertion of nanochannel of bacteriophage SPP1 DNA packaging motor into lipid bilayer via polar hydrophobicity. Biomaterials *105*, 222–227. https://doi.org/10.1016/j.biomaterials.2016.08.002.